Solid State Electronics 147 (2018) 39–43

Contents lists available at ScienceDirect

Solid State Electronics

journal homepage: www.elsevier.com/locate/sse

Lumped-element model of plasmonic solar cells

Chang-Hyun Kim[a,b,*], Maria Seitanidou[c], Jong Woo Jin[a], Yvan Bonnassieux[a], Gilles Horowitz[a], Ioannis Vangelidis[d], Elefterios Lidorikis[d], Argiris Laskarakis[c], Stergios Logothetidis[c]

[a] LPICM, Ecole Polytechnique, CNRS, 91128 Palaiseau, France
[b] Department of Electronic Engineering, Gachon University, Seongnam 13120, Republic of Korea
[c] Laboratory for Thin Films-Nanosystems and Nanotechnology, Department of Physics, Aristotle University of Thessaloniki, Thessaloniki 54124, Greece
[d] Department of Materials Science and Engineering, University of Ioannina, Ioannina 45110, Greece

ARTICLE INFO

The review of this paper was arranged by Y. Kuk

Keywords:
Equivalent circuits
Lumped-element model
Metal nanoparticles
Plasmonics
Solar cells

ABSTRACT

Although metallic nanostructures in solar cells provide versatility in designing useful plasmonic architectures, understanding is still limited on how to exploit their multi-scale contribution as tunable performance. In this article, we suggest a characteristic model that develops into a simple and robust tool for guiding optimization of plasmonic solar devices. The model is conceptually based on the breakdown of the active region into intrinsic and plasmonic sub-circuits, by which the terminal currents are directly correlated with particle geometries and local improvement. Measurements from organic cells support the validity of our theory, and a series of simulation provides further insights into the critical trade-off between voltage and current generation, finally offering a strategy for efficiency enhancement.

1. Introduction

The field of nanotechnology relies on synthesis and control of nanoscale objects that are engineered to undertake active functions in higher-level architectures [1,2]. Therefore, challenges remain on making structures, processes, and interfaces that produce meaningful improvement when embedding nanomaterials into device platforms. Such argument merits special consideration for discussing systems such as plasmonic solar cells [3]. In principle, collective oscillation of electrons in metallic nanostructures dictates substantial amplification of excitation field [4]. However, these effects are strongly localized in nature, and absorption enhancement seen at the device level has been often moderate or highly structure and processing dependent [5,6]. Furthermore, excess metal-semiconductor junctions at plasmonic interfaces are likely to make it harder to extract the maximum of benefits because of simultaneous increase in recombination and quenching losses [7].

Lumped-element modeling is a promising technique to collectively take into account optical, electrical, and structural aspects of plasmonics, providing a means of rational optimization of solar cells [8]. As physical processes are packed into circuit elements, the device operation can be readily visualized to manifest the impact of phenomena on macroscopic measurables (e.g. terminal currents). Also, such a model can serve as a bridge in multi-scale investigation because on one hand, microscopic insights can be obtained through correlation with atomic/molecular-level theories, and on the other hand, larger-scale systems can be predicted by connecting a multitude of cells with necessary components [9]. Equivalent circuits have been previously employed for related topics, proving their powerfulness in tackling diverse scientific questions. Examples include the study of non-ideality in organic solar cells [10], characteristics of nanoplasmonic antennas [11], size effects of perovskite solar cells [12], and single-cell approximation of photovoltaic modules [13].

In this article, we formulate a lumped-element model for the solar cells that include metal nanoparticles (NPs). To pinpoint critical factors affecting plasmonic enhancement, we investigate various sources of positive and negative effects of having NPs in core structures. We first take an inverse modeling approach to reproduce the trends in experimental observations [14], and proceed to simulate hidden aspects of cell behaviors by systematically scanning several parametric dimensions.

2. Experimental methods

Test devices were fabricated using organic semiconductor materials. Clearly, plasmonics brings the possibility of reducing the thickness of semiconductor necessary for light absorption [15], and this implies an economic impact. As one of the organic electronics' targets is low-cost products using roll-to-roll fabrication [16], exploitation of plasmonic effects is in line with the promise of this field. Our devices were

* Corresponding author at: Department of Electronic Engineering, Gachon University, Seongnam 13120, Republic of Korea.
E-mail address: chang-hyun.kim@gachon.ac.kr (C.-H. Kim).

https://doi.org/10.1016/j.sse.2018.06.005
Received 1 December 2017; Received in revised form 27 March 2018; Accepted 8 June 2018

fabricated inside a nitrogen-filled glove box. Anode indium tin oxide (ITO)-coated glass slides were first cleaned by ultrasonication in deionized water, acetone, isopropanol and methanol, and dried on a hot plate. Then, poly(3,4-ethylenedioxythiophene) poly(styrenesulfonate) (PEDOT:PSS) films were deposited by spin coating at 4000 rpm for 30 s onto the substrates and dried on a hot plate at 145 °C for 10 min. Ag NPs were formed by the polyol method [17]. Depending on the target structure, the NPs were spin-coated either on the PEDOT:PSS layer or on the active layer, followed by annealing at 145 °C for solvent evaporation. The active layer was made of the bulkheterojunction of regioregular poly(3-hexylthiophene) (P3HT) (purity of 99.995%) and (6,6)-phenyl C61 butyric acid methyl ester (PCBM) (purity of 99.5%), an architypal system in the organic solar cell technology [18]. The solution of P3HT:PCBM (1:0.8 in weight) was prepared at a total concentration of 50 mg/ml in 1,2-dichlorobenzene. The solution was stirred for over 24 h at 65 °C. The blend was then spin-coated at 1000 rpm for 30 s onto the PEDOT:PSS layer. The devices were finalized by thermal evaporation of the Ca/Al cathode.

3. Results and discussion

3.1. Structural description

The X-ray diffraction (XRD) pattern of Fig. 1(a) indicates that our NPs are geometrically well defined with crystallinity, a remarkable property for solution-processed materials. Also shown in Fig. 1(a) is the atomic-force microscope (AFM) image that visualizes surface distribution of these spin-cast Ag NPs. An approximation is introduced for a uniform two-dimensional (2-D) array of circular islands, as depicted in Fig. 1(b) (top view). Here, l is the diameter of an NP, a is the lattice constant of the unit cell (equivalent to the inter-particle distance), and A is the total active area of a solar cell. This parametrization leads to the definition of several auxiliary values; the single-particle area as $\pi(l/2)^2$, the number of unit cells (= the number of NPs) in the total active area as A/a^2, and the total area occupied by the NPs as $A\pi(l/2a)^2$.

3.2. Current-voltage relationship

Our idea for modeling a solar cell is to consider the current path in the active volume as a network of characteristic impedances. As shown in Fig. 2(a), Z_{int} and Z_{np} correspond to the unit-area impedance of an intrinsic zone and that of an NP zone, respectively. The opto-electronic functionalities in these two regions are supposed to differ substantially, and therefore we regard each region as an effective sub-cell and assign equivalent circuits with independent parameters as shown in Fig. 2(b) and (c) [19]. The current-voltage relationships for these sub-structures are deduced as

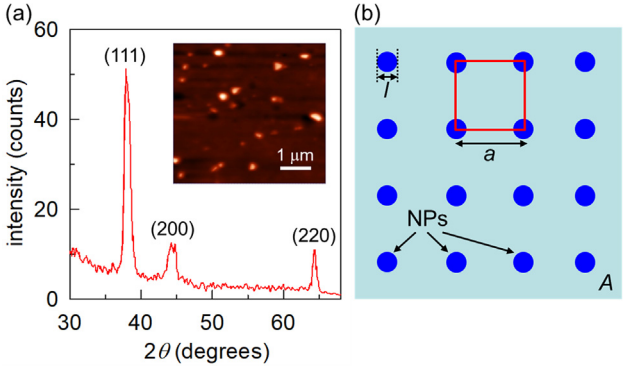

Fig. 1. (a) XRD pattern measured on the Ag NPs deposited on a glass substrate (inset: AFM image of the solution-processed Ag NP arrays). (b) Schematic illustration that parametrizes the two-dimensional spatial distribution of NPs.

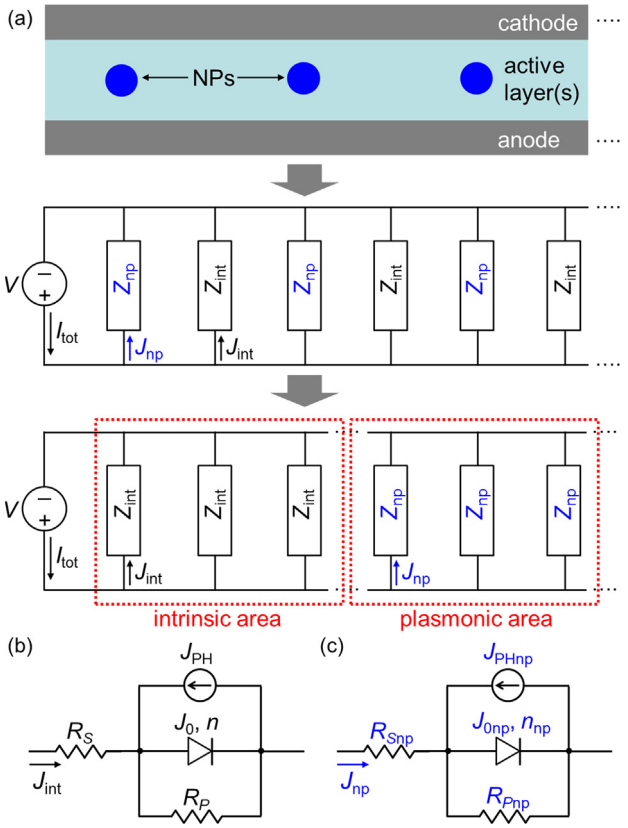

Fig. 2. (a) Description of the lumped-element model. Top: Simplified cross-sectional structure of a solar cell. Middle: Assignment of the intrinsic and plasmonic impedance to the corresponding areas. Bottom: Re-arrangement of parallel branches to sum up the contributions within each characteristic zone. (b) Sub-circuit structure of Z_{int}. (c) Sub-circuit structure of Z_{np}.

$$J_{int} = J_0\left[\exp\left\{\frac{q(V-J_{int}R_S)}{nkT}\right\}-1\right] + \frac{V-J_{int}R_S}{R_P} - J_{PH}, \quad (1)$$

and

$$J_{np} = J_{0np}\left[\exp\left\{\frac{q(V-J_{np}R_{Snp})}{n_{np}kT}\right\}-1\right] + \frac{V-J_{np}R_{Snp}}{R_{Pnp}} - J_{PHnp}. \quad (2)$$

Here, J_{int} is the current density of an intrinsic sub-circuit, with J_0 as the diode saturation current density, n as the diode ideality factor, R_S as the area-multiplied series resistance, R_P as the area-multiplied parallel resistance, and J_{PH} as the photocurrent density. The parameters in Eq. (2) are the counterparts for a plasmonic sub-circuit. As the constituent branches are connected in parallel, they can be re-arranged as two groups [Fig. 2(a) bottom], from which the total current I_{tot} can be constructed as the area-weighted sum of intrinsic and plasmonic current densities. From the notations of Fig. 1, this expression translates into

$$\begin{aligned} I_{tot} &= I_{int} + I_{np} \\ &= J_{int}A\left\{1-\pi\left(\frac{l}{2a}\right)^2\right\} + J_{np}A\pi\left(\frac{l}{2a}\right)^2, \end{aligned} \quad (3)$$

and finally, the total current density J_{tot} is given as

$$J_{tot} = \frac{I_{tot}}{A} = J_{int}\left\{1-\pi\left(\frac{l}{2a}\right)^2\right\} + J_{np}\pi\left(\frac{l}{2a}\right)^2. \quad (4)$$

3.3. Application to real devices

A major feature of our method is the ability to access the pure traits